

See discussions, stats, and author profiles for this publication at: <https://www.researchgate.net/publication/256548914>

Nano-Structured Metal Chalcogenides as Reagents for the Catalytic Carbon-Sulfur Bond Formation in Cross-Coupling Reaction

ARTICLE *in* TOPICS IN CATALYSIS · SEPTEMBER 2013

Impact Factor: 2.37 · DOI: 10.1007/s11244-013-0091-5

CITATIONS

2

READS

46

2 AUTHORS:



Alexey S. Kashin

N. D. Zelinsky Institute of Organic Chemistry

15 PUBLICATIONS 115 CITATIONS

SEE PROFILE



Valentine P. Ananikov

Russian Academy of Sciences

141 PUBLICATIONS 2,841 CITATIONS

SEE PROFILE

Nano-Structured Metal Chalcogenides as Reagents for the Catalytic Carbon–Sulfur Bond Formation in Cross-Coupling Reaction

Alexey S. Kashin · Valentine P. Ananikov

Published online: 25 June 2013
© Springer Science+Business Media New York 2013

Abstract A new approach for the catalytic carbon–sulfur bond formation via cross-coupling reaction is reported. For the first time nano-structured nickel organosulfides $[\text{Ni}(\text{SAr})_2]_n$ were used as a source of SAr groups in catalytic cross-coupling reaction. A unique effect of morphology control of the reactivity of SAr groups in cross-coupling reaction was found. Synthesized nano-structured particles were characterized by field-emission scanning electron microscopy and their reactivity was studied by NMR in solution. Cross-coupling reaction with Cu catalyst was shown to proceed in the liquid phase and involve leaching, whereas the reaction with Pd catalyst is more complex and may involve both—homogeneous and heterogeneous pathways.

Keywords Metal chalcogenides · Nanoparticles · C–S bond formation · Catalysis · Cross-coupling · Field-emission SEM

1 Introduction

Over the last few decades transition-metal catalyzed transformations became a conventional tool for the buildup of carbon skeleton and for the introduction of heteroatoms in organic molecules. These reactions play an outstanding role in the organic synthesis due to their excellent selectivity and tolerance to wide range of functional groups [1–4]. One of the important applications of the carbon–heteroatom bond

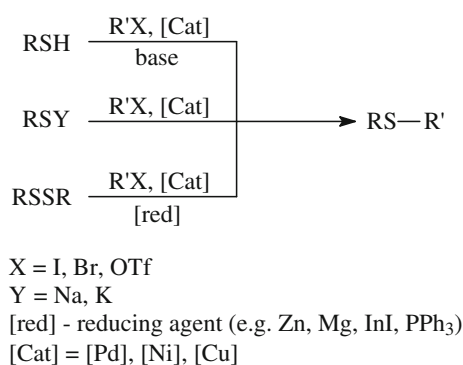
formation reactions is the preparation of sulfur-containing compounds, which are of great demand in the pharmaceutical industry and in material science application [5–7].

The majority of the existing methods for the C–S cross-coupling can be divided into three groups according to the source of SR building blocks: reactions with thiols, thiolates and disulfides (Scheme 1). A number of catalytic systems involving Pd, Ni, Cu and other metals have been reported and the topic was recently reviewed [8–11].

We propose that metal chalcogenides can be perspective reagents to extend the scope of carbon–heteroatom cross-coupling reactions. An important advantage is the possibility to control reactivity at nano-structured level by changing size and shape of the particles. Metal chalcogenides are the well-known type of nanoparticles, where metal atoms are linked with non-metallic atoms such as sulfur or selenium. A variety of metal chalcogenide nanoparticles have found numerous applications in nanotechnology, microelectronics, optics and material science [12–19]. However, in spite of such outstanding development in the area of nanotechnology, application of nano-sized metal chalcogenides in catalysis and organic synthesis remains largely unexplored [20–22].

In the present work we report the first example of transition metal nanoparticles utilization as reagents for the carbon–sulfur bond formation reactions. For this purpose we have used metal chalcogenides that contain organic groups in the core of the nanoparticle (“nanosalts”) [23]. These nano-structured chalcogen-containing salts can be easily prepared by the reaction between nickel acetylacetonate and aryl thiols resulting in chain-like structures, where nickel atoms are linked by μ^2 -SR groups. It was demonstrated that these chains can be assembled into nanoparticles due to the self-organization process [23–25] and resulting in nanoparticles of coordination polymer (Scheme 2). Such transition from

A. S. Kashin · V. P. Ananikov (✉)
N. D. Zelinsky Institute of Organic Chemistry, Russian
Academy of Sciences, Leninsky Prospekt 47,
Moscow 119991, Russia
e-mail: val@ioc.ac.ru

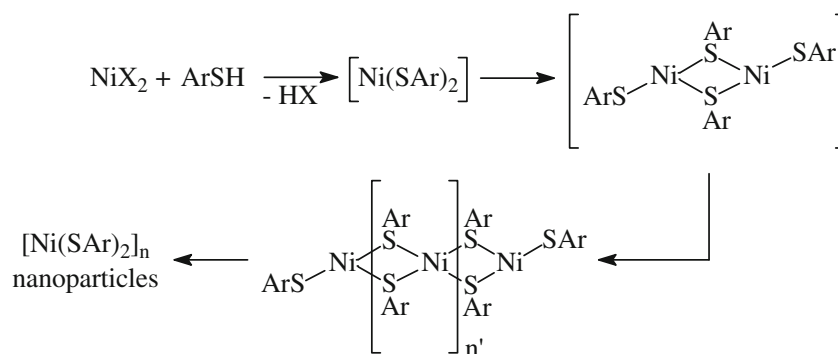
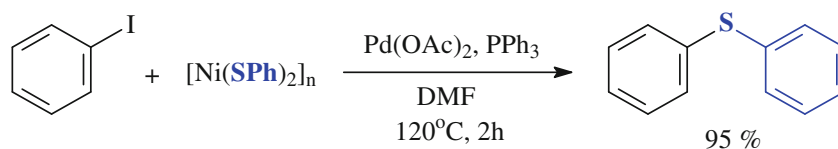
**Scheme 1** C–S bond formation via cross-coupling reactions

routine metal chalcogenides to advanced polymeric materials incorporating metal-SR moieties gives us novel interesting reagent for the carbon–sulfur bond formation.

2 Results and Discussion

$[\text{Ni}(\text{SPh})_2]_n$ nanoparticles were synthesized according to the literature method [23, 24] and then were treated with stoichiometric quantity of iodobenzene in DMF at 120 °C. After 2 h of heating there were no noticeable changes in the ^1H and $^{13}\text{C}\{^1\text{H}\}$ NMR spectra of the reaction mixture. Under these conditions we were not able to obtain the desired product.

To promote the cross-coupling reaction we have added catalytic amounts of PPh_3 and palladium acetate. Besides the fact that palladium itself can serve as a catalyst, Pd/ PPh_3 system can also promote controlled release of reactive sulfur species from the “nanosalts” chains due to the ligand substitution, transmetallation or partial detachment.

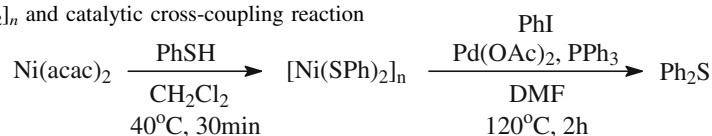
Scheme 2 Formation of the $[\text{Ni}(\text{SAr})_2]_n$ nanoparticles (“nanosalts”)**Scheme 3** Reaction of $[\text{Ni}(\text{SPh})_2]_n$ with PhI in the presence of catalytic amounts of $\text{Pd}(\text{OAc})_2$ and PPh_3 

Using 5 mol% of $\text{Pd}(\text{OAc})_2$ and 20 mol% of PPh_3 the cross-coupling reaction proceeded smoothly and the product yield determined by NMR was about 95 % (Scheme 3). It should be noted that the reaction required both—palladium salt and phosphine ligand. When we used only one of the components (either $\text{Pd}(\text{OAc})_2$ or PPh_3) no reaction was observed.

Nickel thiophenolate complex used as a reagent for the cross-coupling reaction was synthesized from nickel acetylacetonate and thiophenol. As we mentioned above, initially synthesis of $[\text{Ni}(\text{SPh})_2]_n$ was carried out using literature procedure which utilized a 100-fold excess of thiophenol. We have studied the influence of the $\text{PhSH}:\text{Ni}(\text{acac})_2$ ratio on the synthesis of $[\text{Ni}(\text{SPh})_2]_n$ nanoparticles and finally on their reactivity in C–S cross-coupling reaction. Three samples of the $[\text{Ni}(\text{SPh})_2]_n$ nanoparticles prepared with the usage of 2, 10 or 20 equiv. of thiol were examined in the reaction with iodobenzene in the presence of palladium acetate and triphenylphosphine (Table 1).

Indeed, only 36 % yield of the cross-coupling product was observed using the $[\text{Ni}(\text{SPh})_2]_n$ material prepared with stoichiometric amount of reagents (entry 1, Table 1). An increase of the $\text{PhSH}:\text{Ni}(\text{acac})_2$ ratio to 10 gave better yield of 80 % (entry 2, Table 1), whereas usage of 20 equiv. of thiophenol resulted in the high yield of 90 % (entry 3, Table 1). Further increase of the ratio gave only a minor influence on the product yield (entry 4, Table 1).

Field-emission scanning electron microscopy (FE-SEM) analysis of the synthesized complexes showed that the excess of thiophenol facilitated the formation of the small shaped particles with characteristic diameter about 100–300 nm incorporated into micro-sized (several μm in size) aggregates (Fig. 1c). Decreasing the amount of PhSH

Table 1 Synthesis of $[\text{Ni}(\text{SPh})_2]_n$ and catalytic cross-coupling reaction

Entry	Equiv. of PhSH ^a	Ph ₂ S yield ^b (%)
1	2	36
2	10	80
3	20	90
4	100	95

^a On the first step of $[\text{Ni}(\text{SPh})_2]_n$ nanoparticles preparation from $\text{Ni}(\text{acac})_2$

^b The yield on the second step of catalytic cross-coupling reaction determined by NMR

gave particles of larger size (Fig. 1b) or not structured material (Fig. 1a). It should be noted that the studied samples have exactly the same composition of $[\text{Ni}(\text{SPh}_2)]_n$, while differ only in morphology of the particles. Very likely, the driving force for the small particles formation is kinetics—the excess of thiophenol facilitated rapid nucleation, which led to the formation of smaller particles.

To summarize, it is evident that the reactivity of synthesized “nanosalts” strongly depends on their morphology. One of the possible explanations of this phenomenon is that the formation of small uniformly shaped particles provided high surface/volume ratio—a limiting factor for the heterogeneous reactions in solution. The second possible influence is the increase in the ratio of $\mu^1\text{-SR}/\mu^2\text{-SR}$ groups upon decrease of the nanoparticle size (smaller chains in the coordination polymer). It was demonstrated that $\mu^1\text{-SR}$ groups are more reactive towards alkyne as compared to the $\mu^2\text{-SR}$ groups [25]. For our further experiments we used $[\text{Ni}(\text{SPh})_2]_n$ nanoparticles prepared with 20 equiv. of thiophenol (Fig. 1c). Application of an excess of thiophenol for the synthesis of the nanoparticles is not an obstacle from economic reasons, since the remaining thiol can be easily recovered and re-used. The presence of an excess of the thiol was important to maintain required morphology of the nanoparticles in order to ensure high reactivity in the catalytic reaction.

Although the catalytic system with 5 mol% of $\text{Pd}(\text{OAc})_2$ gave high product yield, such catalyst loadings of palladium are impractical. Twofold decrease of $\text{Pd}(\text{OAc})_2$ amount to 2.5 mol% led to significant loss in the reaction yield (cf. entries 1 and 2, Table 2). A number of experiments showed that copper salts were the appropriate substitute for the palladium salt (entries 3–10, Table 2). Widely used diamino ligand TMEDA allowed to achieve the yield of 56 % with 10 mol% of $\text{Cu}(\text{OAc})_2$ (entry 8, Table 2). However, cross-coupling reaction in the $\text{Cu}(\text{OAc})_2/\text{TMEDA}$ catalytic system was accompanied by the side-reaction leading to formation of undesired Ph_2S_2 by-product. The best results were

found with the catalytic system containing copper acetate in the presence of triphenylphosphine ligand (entry 10, Table 2). The reaction yield of 82 % was achieved (10 mol%, 120 °C, 6 h), which is comparable to the reaction mediated by Pd catalyst (5 mol%, 120 °C, 2 h) as shown in Table 2 (entries 1 and 10).

We have also obtained preliminary data on the influence of organic substituent in the SAR group on the reactivity of $[\text{Ni}(\text{SAR})_2]_n$ nanoparticles. Different nickel “nanosalts” were prepared, characterized by FE-SEM (Fig. 2) and examined in the reaction with iodobenzene (Table 3).

As it may be expected, nickel “nanosalt” particles with no specific shape (Fig. 2a) had low activity in the reaction with iodobenzene (entry 2, Table 3). Nickel “nanosalt” containing *p*- $\text{BrC}_6\text{H}_4\text{S}$ - groups formed the uniformly shaped particles with unprecedented pattern (Fig. 2b). The mean diameter of the particles was about 4 μm and the unique biconcave disks morphology was observed (Fig. 2b). More detailed morphology examination revealed the complex layered structure. Thickness of the biconcave disks varies from 100 nm (several individual layers) to 1 μm . This “nanosalt” gave high yield in the catalytic cross-coupling reaction (entry 3, Table 3). In case of “nanosalt” containing *o*- $\text{CH}_3\text{C}_6\text{H}_4\text{S}$ - groups the yield of sulfide product was lower than in case of *p*- $\text{CH}_3\text{C}_6\text{H}_4\text{S}$ - group (entries 2 and 4, Table 3). This effect can be attributed to steric influence of the *o*- CH_3 substituent on the studied reaction. An interesting effect was observed using *o*- $\text{NH}_2\text{C}_6\text{H}_4\text{S}$ - groups in the metal chalcogenide—this nickel material showed no reactivity towards iodobenzene (entry 5, Table 3). The most probable explanation of this inactivity is a strong chelating interaction involving *o*-positioned thiol and amino-groups, which led to formation of stable resting states and deteriorated catalytic activity completely.

Proposed mechanism of the catalytic cycle involves oxidative addition of Ar'I , transmetalation involving $[\text{Ni}(\text{SAR})_2]_n$ followed by reductive elimination (Scheme 4). We have performed EDX-SEM study of the solid phase in

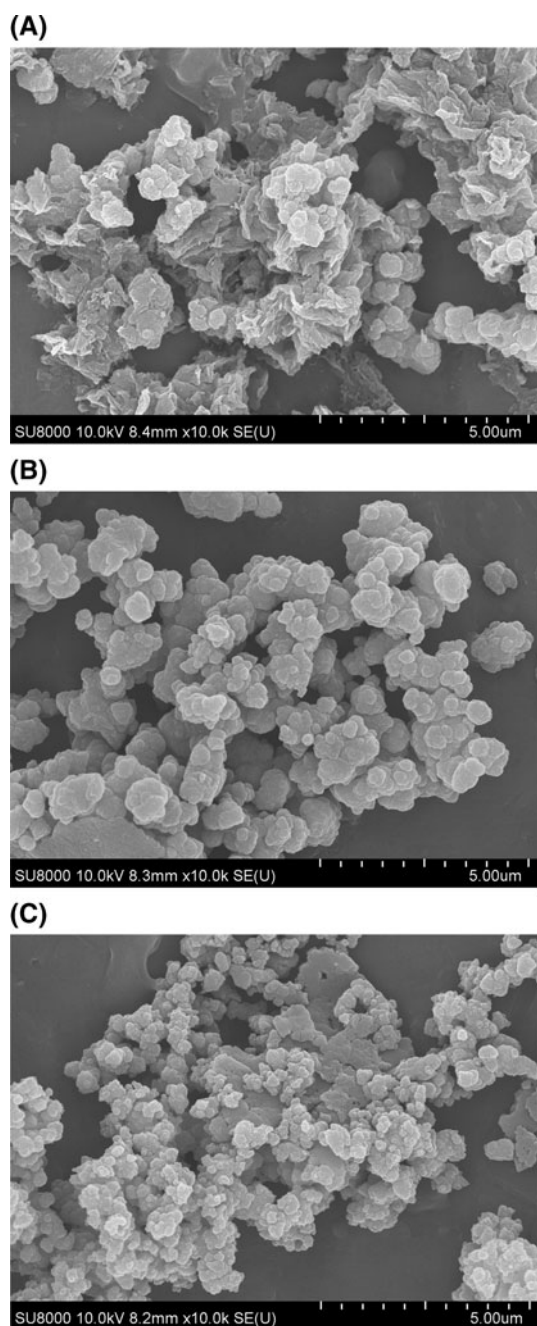


Fig. 1 The morphology of the particles formed upon reaction of $\text{Ni}(\text{acac})_2$ with: 2 equivalents of PhSH (a), 10 equivalents of PhSH (b), 20 equivalents of PhSH (c)

order to investigate the reaction mechanism. Freshly prepared $[\text{Ni}(\text{SPh})_2]_n$ was introduced into the reaction with iodobenzene in the presence of triphenylphosphine and metal salt additives (copper or palladium catalysts). Samples of the solid phases taken from the reaction mixtures at 30 % conversion and after completion of the reaction were thoroughly washed and dried under reduced pressure.

In the case of Pd catalyst EDX-SEM study has shown that the surface of the solid $[\text{Ni}(\text{SPh})_2]_n$ particles also

contained palladium. The amount of palladium continuously rose during the reaction up to 20 mol% against the sum of nickel and palladium. This fact may indicate coordination of Pd to the nanoparticles and operation of the catalytic cycle on the surface of the particles. Another possible option is degradation and precipitation of palladium during the course of the reaction in solution.

Different picture was observed in the case of copper catalyst: there were no copper x-ray lines in the spectrum, surface of the solid phase of the reaction mixture contained nickel as the only metallic component. The fact suggests that copper is not attached to the surface of nano-structured $[\text{Ni}(\text{SPh})_2]_n$ neither during the transformation nor after completion the reaction. Since the copper species were presented in the liquid phase, the catalytic reaction proceeds in solution and involves leaching of the $\text{Ni}(\text{SPh})_2$ units. A similar mechanistic framework may be expected with the difference in the nature of nickel species involved in transmetallation step (Scheme 4; $n = 1\text{--}3$ for leaching of small complexes and reaction in solution).

At the final stage of the reaction in the cases of high values of conversion (Table 2, entries 1 and 10) the $[\text{Ni}(\text{SAr})_2]_n$ reagent was consumed and converted to NiI_2 , whereas the arylthio group was incorporated into the final ArSAr' product (Scheme 4). In the cases of incomplete conversion corresponding amounts of coordinated sulfur polymer remained unreacted.

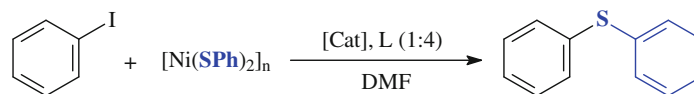
To summarize, we have demonstrated that metal chalcogenide nanoparticles— $[\text{Ni}(\text{SPh})_2]_n$ (nanoparticles of coordination polymer)—are useful reagents in catalytic C–S cross-coupling reactions with Pd and Cu catalysts. A unique effect of morphology control of the SAr group donor reactivity in cross-coupling reaction was found. Cross-coupling reaction with Cu catalyst was shown to proceed in the liquid phase and involve leaching, whereas the same reaction with Pd catalyst is more complex and may involve both—homogeneous and heterogeneous pathways.

The aim of the present study was to demonstrate the possibility to enhance the reactivity of metal chalcogenide in cross-coupling reaction by adjusting particle size and shape. We anticipate further studies on the subject to investigate scope and synthetic utility of this approach.

3 Experimental

3.1 General Considerations

NMR spectra were recorded on Bruker DRX-500 spectrometer with working frequencies 500.1 and 125.8 MHz for ^1H and ^{13}C , respectively. The products ArSAr' shown

Table 2 Catalytic activity of Pd and Cu in the studied cross-coupling reaction

Entry	Catalyst (mol%)	Ligand (L)	Reaction conditions	Ph ₂ S yield ^a (%)
1	Pd(OAc) ₂ (5)	PPh ₃	120 °C, 2 h	90
2	Pd(OAc) ₂ (2.5)	PPh ₃	120 °C, 2 h	19
3	Cu(OAc) ₂ (10)	–	120 °C, 2 h	27 ^b
4	Cu(OAc) ₂ (10)	–	120 °C, 6 h	33 ^b
5	Cu(OAc) ₂ (5)	TMEDA	120 °C, 2 h	32 ^b
6	CuCl (5)	TEEDA	120 °C, 2 h	19 ^b
7	Cu(OAc) ₂ (10)	TMEDA	120 °C, 2 h	52 ^b
8	Cu(OAc) ₂ (10)	TMEDA	120 °C, 6 h	56 ^b
9	Cu(OAc) ₂ (10)	PPh ₃	120 °C, 2 h	37
10	Cu(OAc) ₂ (10)	PPh ₃	120 °C, 6 h	82

^a Determined by NMR^b Ph₂S₂ was formed as a by-product in 20–30 % yield

in Table 3 were identified according to the published data [26].

3.1.1 Determination of Reaction Yields by NMR

The yields were measured based on ¹³C{¹H} NMR spectra. Inverse gate WALTZ-16 broadband proton decoupling was used for ¹³C{¹H} NMR spectra, the free induction decays (FIDs) were processed by performing an exponential weighting (LB = 3 Hz) before Fourier transformation. ¹³C{¹H} NMR spectra were acquired with a relaxation delay of 5 s.

3.2 FE-SEM Measurements

The powder samples were disposed onto the surface of aluminum foil from the suspension in acetone. Small pieces of foil containing the powder were mounted on a 25 mm aluminum specimen stub and fixed by double-sided carbon tape. Metal coating with a thin film (20 nm) of platinum/palladium alloy (80/20) was performed using magnetron sputtering method as described earlier [27]. The observations were carried out using a Hitachi SU8000 field-emission scanning electron microscope (FE-SEM). Images were acquired in secondary electron mode at 10 kV accelerating voltage and at working distance of 8–10 mm. Morphology of the coated samples was studied adjusted for the metal coating surface effects.

EDX-SEM studies were carried out using Oxford Instruments X-max EDX system. For the quantitative analysis

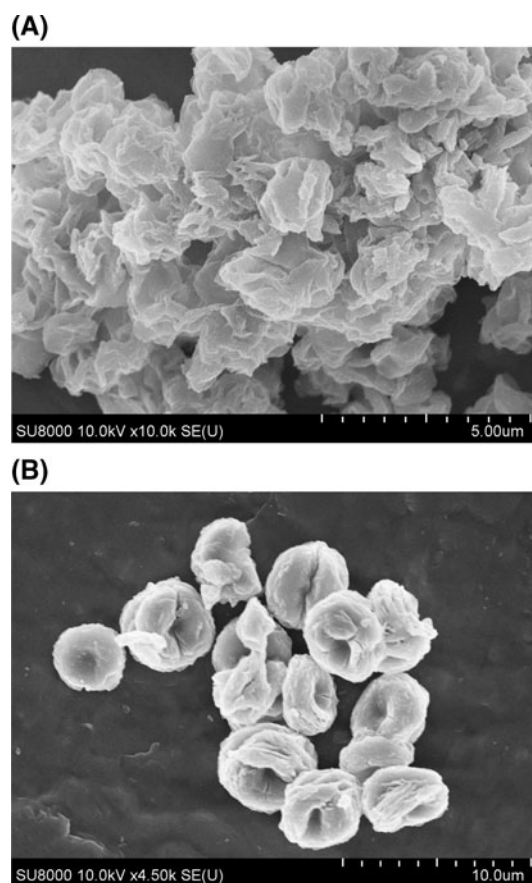
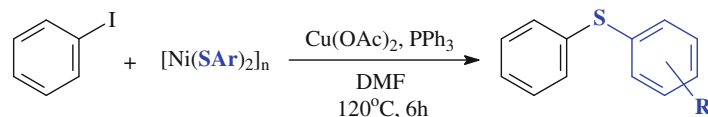
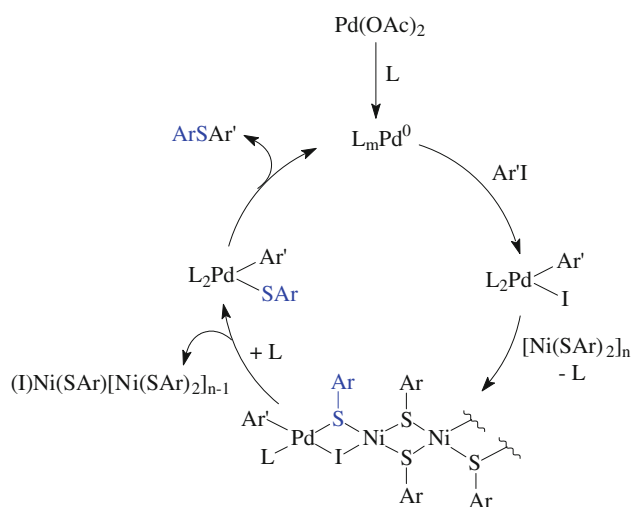


Fig. 2 The morphology of the nickel “nanosalt” particles formed upon reaction of Ni(acac)₂ with: *p*-CH₃C₆H₄SH (a) and *p*-BrC₆H₄SH (b)

Table 3 Cu-catalyzed reaction with various nickel “nanosalts”

Entry	R	Product	Yield ^a (%)
1	H		82
2	<i>p</i> -CH ₃		45
3	<i>p</i> -Br		86
4	<i>o</i> -CH ₃		20
5	<i>o</i> -NH ₂		0

^a Determined by NMR**Scheme 4** Plausible mechanism for the Pd-catalyzed reaction

internal standards were used after calibration. Before the measurements all samples were coated with a thin film (10 nm) of carbon using Cressington 208 carbon coater.

3.3 Synthesis of the Nickel [Ni(SAr)₂]_n Particles

Freshly dried Ni(acac)₂ (308.3 mg; 1.2 mmol) was dissolved in 6 mL of CH₂Cl₂. Then, under vigorous stirring 20-fold excess of thiol (24 mmol) was added dropwise to the resulting solution as a neat liquid in case of thiophenol or 2-methylbenzenethiol or as a saturated solution in CH₂Cl₂ in case of other thiols. The precipitate was formed upon addition. Stirring was continued for 30 min at 40 °C. The product was isolated by centrifugation (3,500 rpm, 5 min), washed five times with 10 mL of acetone and dried under reduced pressure.

In case of *p*-CH₃C₆H₄SH the particles were too small to be separated by centrifugation. Precipitation was induced by dilution of the reaction mixture with 5 mL of acetone.

[Ni(SPh)₂]_n. Dark violet solid. Yield: 99 %.

[Ni(S-*p*-CH₃C₆H₄)₂]_n. Dark brown solid. Yield: 40 %.

[Ni(S-*p*-BrC₆H₄)₂]_n. Black solid. Yield: 91 %.

[Ni(S-*o*-NH₂C₆H₄)₂]_n. Yellow solid. Yield: 93 %.

[Ni(S-*o*-CH₃C₆H₄)₂]_n. Brown solid. Yield: 93 %.

3.4 Synthesis of $[\text{Ni}(\text{SPh})_2]_n$ Particles with Various Amounts of Thiophenol and Their Reaction with Iodobenzene (Table 1)

Freshly dried $\text{Ni}(\text{acac})_2$ (51.4 mg; 0.2 mmol) was dissolved in 1 mL of CH_2Cl_2 . Then, under vigorous stirring twofold, tenfold and 20-fold excess of thiophenol (0.041 mL, 0.4 mmol; 0.204 mL, 2 mmol and 0.409 mL, 4 mmol, respectively) was added dropwise to the resulting solution. The precipitate was formed upon addition. Stirring was continued for 30 min at 40 °C. The product was isolated by centrifugation (3,500 rpm, 5 min), washed four times with 4 mL of hexanes and dried under reduced pressure. Then, the solid substance obtained was transferred into a 5-mL glass tube fitted with a magnetic stirrer bar. $\text{Pd}(\text{OAc})_2$ (4.5 mg, 0.02 mmol), triphenylphosphine (21 mg, 0.08 mmol), DMF (1 mL) and iodobenzene (0.045 mL, 82 mg, 0.4 mmol) were added sequentially into the tube. The reaction vessel was flushed with argon and sealed with a screw cap. The reaction mixture was stirred at 120 °C for 2 h. After completion of the reaction solid phase was removed by centrifugation (3,500 rpm, 5 min) and liquid phase was analyzed by NMR.

3.5 Reactions of $[\text{Ni}(\text{SPh})_2]_n$ with Various Catalyst Precursors (Table 2)

The metal salt (see Table 2), ligand (for PPh_3 only, see Table 2) and $[\text{Ni}(\text{SPh})_2]_n$ (55.4 mg, 0.2 mmol) were added to a 5-mL glass tube fitted with a magnetic stirrer bar. Then, the tube was charged with DMF (1 mL); iodobenzene (0.045 mL, 82 mg, 0.4 mmol) and ligand (for TMEDA or TEEDA, see Table 2) were added to the resulting suspension. The reaction vessel was flushed with argon and sealed with a screw cap. The reaction mixture was stirred at 120 °C for 2 or 6 h (see Table 2). After completion of the reaction solid phase was removed by centrifugation (3,500 rpm, 5 min) and liquid phase was analyzed by NMR.

3.6 Catalytic Reaction Between $[\text{Ni}(\text{SAr})_2]_n$ Particles and Iodobenzene (Table 3)

$\text{Cu}(\text{OAc})_2$ (18 mg, 0.1 mmol), triphenylphosphine (105 mg, 0.4 mmol) and nickel particles (0.5 mmol) were added to a 20-mL glass tube fitted with a magnetic stirrer bar. Then, the tube was charged with DMF (3 mL). The iodobenzene (0.111 mL, 204 mg, 1 mmol) was added to the resulting suspension. The reaction vessel was flushed with argon and

sealed with a screw cap. The reaction mixture was stirred at 120 °C for 6 h. After completion of the reaction solid phase was removed by centrifugation (3,500 rpm, 5 min) and liquid phase was analyzed by NMR.

Acknowledgments The work was supported in part by the Russian Foundation for Basic Research (Projects No. 13-03-01210 and 12-03-31512), grant MD-4969.2012.3, the Ministry of education and science of Russian Federation (Project 8453) and Programs of Division of Chemistry and Material Sciences of RAS.

References

1. Negishi E (ed) (2002) Handbook of organopalladium chemistry for organic synthesis. Wiley, New York
2. Diederich F, Stang PJ (eds) (2004) Metal-catalyzed cross-coupling reactions. Wiley-VCH, Weinheim
3. Nicolaou KC, Sorensen EJ (eds) (1996) Classics in total synthesis. Wiley-VCH, Weinheim
4. Nicolaou KC, Snyder SA (eds) (2003) Classics in total synthesis II. Wiley-VCH, Weinheim
5. Cremling RJ (1996) An introduction to organosulfur chemistry. Wiley, Chichester
6. Bernardi F, Csizmadia IG, Mangini A (eds) (1985) Organic sulfur chemistry: theoretical and experimental advances, vol 19. Elsevier, Amsterdam
7. Block E (1978) Reactions of organosulfur compounds. Academic Press, New York
8. Eichman CC, Stambuli P (2011) Molecules 16:590–608
9. Bichler P, Love JA (2010) Top Organomet Chem 31:39–64
10. Beletskaya IP, Ananikov VP (2011) Chem Rev 111:1596–1636
11. Hartwig JF (2008) Acc Chem Res 41:1534–1544
12. Wang L, Zhu Y, Li H, Li Q, Qian Y (2010) J Solid State Chem 183:223–227
13. Barry L, Holmes JD, Otway DJ, Copley MP, Kazakova O, Morris MA (2010) J Phys: Condens Matter 22:076001
14. Huang S, Harris KDM, Lopez-Capel E, Manning DAK, Rickard D (2009) Inorg Chem 48:11486–11488
15. Diaz-Chao P, Ferrer IJ, Ares JR, Sanchez C (2009) J Phys Chem C 113:5329–5335
16. Shemesh Y, Macdonald JE, Menagen G, Banin U (2011) Angew Chem Int Ed 50:1185–1189
17. Sines IT, Schaak RE (2011) J Am Chem Soc 133:1294–1297
18. Gao M-R, Jiang J, Yu S-H (2012) Small 8:13–27
19. Sokolov MN, Abramov PA (2012) Coord Chem Rev 256:1972–1991
20. Chan SL-F, Low K-H, So GK-M, Chui SS-Y, Che C-M (2011) Chem Commun 47:8808–8810
21. Jain VK, Jain L (2010) Coord Chem Rev 254:2848–2903
22. Dey S, Jain VK (2004) Platinum Metals Rev 48:16–29
23. Ananikov VP, Beletskaya IP (2011) Dalton Trans 40:4011–4023
24. Ananikov VP, Orlov NV, Beletskaya IP (2006) Organometallics 25:1970–1977
25. Ananikov VP, Orlov NV, Zaleskiy SS, Beletskaya IP, Khrustalev VN, Morokuma K, Musaev DG (2012) J Am Chem Soc 134:6637–6649
26. Taniguchi N (2007) J Org Chem 72:1241–1245
27. Kashin AS, Ananikov VP (2011) Russ Chem Bull 60:2602–2607